Neurobiology of Disease 140 (2020) 104812

Contents lists available at ScienceDirect

Neurobiology of Disease

journal homepage: www.elsevier.com/locate/ynbdi

JNK signaling activation in the Ube3a maternal deficient mouse model: its specific inhibition prevents post-synaptic protein-enriched fraction alterations and cognitive deficits in Angelman Syndrome model

Clara Alice Musi[a,b], Graziella Agrò[b], Lucia Buccarello[a,b], Serena Camuso[b], Tiziana Borsello[a,b,*]

[a] Department of Pharmacological and Biomolecular Sciences, Milan University, Italy
[b] Department of Neuroscience, Istituto di Ricerche Farmacologiche Mario Negri-IRCCS, Milan, Italy

ARTICLE INFO

Keywords:
Neurodevelopmental disease
C-Jun-N-terminal-kinase
MAP-kinase stress pathway
Synaptic dysfunction
Neuroprotection
D-JNKI1

ABSTRACT

Deficiency of the E3 ubiquitin ligase UBE3A leads to the neurodevelopmental disorder Angelman syndrome (AS), while higher levels are linked to autism spectrum disorder. The mechanisms underlying the downstream effects of UBE3A loss or gain of function in these disorders are still not well understood, and treatments are still lacking.

Here, using the *Ube3a* maternal loss (*Ube3a* $^{m-/p+}$) mouse model, we report an important JNK signaling activation in the hippocampus, cortex and cerebellum correlating with the onset of behavioral defects and biochemical marker alterations in the post-synaptic element, suggesting important spine pathology. JNK activation occurs at 7 and persists up till 23 weeks in *Ube3a* $^{m-/p+}$ mice in two different cellular compartments: the nucleus and the post-synaptic protein-enriched fraction.

To study JNK's role in *Ube3a* $^{m-/p+}$ pathology we treated mice with the specific JNK inhibitor peptide, D-JNKI1, from 7 to 23 weeks of age. Preventing JNK action in vivo restores the post-synaptic protein-enriched fraction defects and the cognitive impairment in these mice. Our results imply a critical role of UBE3A-JNK signaling in the pathogenesis of UBE3A-related disorders. In particular, it was clear that JNK is a key player in regulating AS synaptic alterations and the correlated cognitive impairments, in fact, its specific inhibition tackles *Ube3a* $^{m-/p+}$ pathology.

This study sheds new light on the neuronal functions of UBE3A and offers new prospects for understanding the pathogenesis of UBE3A-related disorders.

1. Introduction

Deletions or loss-of-function mutations in the maternal allele of the UBE3A gene lead to Angelman syndrome (AS), a developmental neurological disorder in the Autism spectrum characterized by severe intellectual disability. The consequences of *UBE3A* dysfunction/loss and the mechanisms of the downstream effects of this gain or loss of functions are still not fully understood, and effective treatments are lacking. The AS mouse model, with loss of the *Ube3a* (*Ube3a*$^{m-/p+}$) maternal allele, recapitulates many of the AS's symptoms, including motor and cognitive impairments closely correlated with reduced spine number and aberrant spine morphology (Dindot et al., 2008; Jana, 2012; Jiang et al., 1998; Kim et al., 2016; Koyavski et al., 2019; Yashiro et al., 2009).

UBE3A appears to have a critical role in dendritic spine development and in their plasticity (Kim et al., 2016; Yashiro et al., 2009). In addition, *Ube3a* $^{m-/p+}$ mice also have defective hippocampal long-term potentiation and dendritic spine density, in line with deficits in behavioral tasks (Dindot et al., 2008; van Woerden et al., 2007). However, little is known about the neuronal function of the UBE3A in control condition and even less about the pathogenesis linked to UBE3A-related disorders. UBE3A plays a role in dendritic spine function/dysfunction, but the mechanisms that link E3 ubiquitin ligase UBE3A to dendritic spine are not clear yet.

To identify downstream effectors of UBE3A loss-of-function we studied the stress-JNK signaling pathway in *Ube3a* $^{m-/p+}$ mice. Since c-Jun-N-terminal Kinase (JNK) signaling is an intracellular pathway strongly responsive in the brain to different stressors and plays a key role in brain development and maintenance (Antoniou and Borsello, 2010; Coffey, 2014), we investigated whether the JNK pathway was involved in AS and in particular in AS synaptic dysfunction. JNK controls neuronal plasticity and memory formation (Coffey, 2014; Kumar

* Corresponding author at: Professor of Human Anatomy, Neuronal Death and Neuroprotection Lab, Department of Pharmacological and Biomolecular Sciences, CEND-Center of Excellence on Neurodegenerative Diseases, Università degli Studi di Milano, Via Balzaretti 9, 20133 Milano, Italy.
E-mail addresses: tiziana.borsello@unimi.it, tiziana.borsello@marionegri.it (T. Borsello).

https://doi.org/10.1016/j.nbd.2020.104812
Received 28 November 2019; Received in revised form 30 January 2020; Accepted 18 February 2020
Available online 19 February 2020

et al., 2015), synaptic functions and synaptic dysfunction (Biggi et al., 2017; Buccarello et al., 2017, 2018; Sclip et al., 2011, 2013, 2014). The JNK signaling pathway is activated in many different brain diseases such as stroke (Borsello et al., 2003; Vercelli et al., 2015), epilepsy (Auladell et al., 2017; Zhuo et al., 2016), Alzheimer's (Colombo et al., 2009; Okazawa and Estus, 2002; Ploia et al., 2011; Sclip et al., 2011, 2014), Parkinson's (Kuan and Burke, 2005; Wang et al., 2014; Wang et al., 2004), Huntington's disease (Perrin et al., 2009) and Spinal Muscular Atrophy (Schellino et al., 2018). Less is known about JNK's function in neurodevelopmental diseases, so we investigated this in the AS *Ube3a* $^{m-/p+}$ mouse model.

Ube3a$^{m-/p+}$ mice present significant activation of the JNK signaling pathway in the whole homogenate and in the synaptic protein-enriched fraction compared to age-matched wild-type (wt) mice, indicating stress mediated by JNK in the cortex, hippocampus and cerebellum already at 7 weeks of age, early in the pathology. JNK activation persists up to 23 weeks of age, when the disorder is more severe, suggesting long-lasting activation of this stress pathway. *Ube3a*$^{m-/p+}$ mice also show a change in PSD biochemical marker levels related to JNK activation and behavioral deficits, suggesting an altered cytoarchitecture of the dendritic spines.

Synaptic injury is the first neurodegenerative event in brain diseases and understanding the molecular players leading to synaptic dysfunction will help in the development of tailored synapse-targeted therapies for neurodevelopmental disorders.

Here we identify JNK as an important kinase that regulates synaptic injury downstream UBE3A loss-of-function in *Ube3a*$^{m-/p+}$ mice.

Inhibition of JNK signaling activation in *Ube3a*$^{m-/p+}$ mice, by chronic treatment with the specific JNK inhibitor D-JNKI1, prevents post-synaptic protein-enriched alterations. The treatment significantly rescued cognitive deficits in the *Ube3a*$^{m-/p+}$ mice and partially reversed some of the locomotor impairments.

In summary, this study identifies JNK as an important player regulating synaptic damage in *Ube3a*$^{m-/p+}$ mice, suggesting that JNK is a potential target for therapeutic intervention in UBE3A-related disorders.

2. Material and methods

2.1. Animal procedures

We used a model of Angelman Syndrome (Jiang et al., 1998) B6.129S7-Ube3a < tm1Alb > /J - The Jackson Laboratory on a C57BL/6 background and age-matched wild-type mice (C57BL/6) served as controls. Heterozygous Ube3atm1Alb females were bred with wt males; this resulted in maternal transmission of the Ube3a mutant allele and paternal transmission of the imprinted/silenced wt allele. Genotyping was done by PCR using a protocol provided by Jackson Laboratory.

Mice were bred at the IRCCS Mario Negri Institute for Pharmacological Research in a specific-pathogen-free (SPF) facility with regular 12:12 h light/dark cycles (lights on 07:00 a.m.), at constant room temperature of 22 ± 2 °C, and relative humidity 55 ± 10%. Animals were housed (4 per group) in individually ventilated cages, with water and food ad libitum.

Procedures involving animals and their care were in accordance with national and international laws and policies (EU Directive 2010/63/EU for animal experiments). The Mario Negri Institute for Pharmacological Research (IRCCS, Milan, Italy) Animal Care and Use Committee (IACUC) approved the study, which was conducted according to the institutional guidelines, in compliance with Italian law. The scientific project was approved by the Italian Ministry of Health (Permit Number 565/2017-PR).

The experimental scheme comprised four groups: untreated wt and *Ube3a* $^{m-/p+}$ mice, D-JNKI1 treated wt and *Ube3a* $^{m-/p+}$ mice. For behavioral tests we used male and female mice, in particular 30 wt mice, 30 *Ube3a* $^{m-/p+}$ mice; for biochemical analysis (TIF and Western blots) we analyzed male and female mice as well, 10 mice per group.

2.2. Animal treatment

All mice (*Ube3a*$^{m-/p+}$ or wt) were injected intraperitoneally (ip) with D-JNKI1 (22 mg/kg) every 28 days from 7 to 23 weeks of age. Their weight was recorded before and after each dose. Mice were always treated at the same time of day (9:00–10:00 a.m.) in randomized order in a specific room inside the animal facility. Each single mouse was our experimental unit. After behavioral tests the animals were euthanized and brains were dissected for biochemical analysis.

2.3. Behavioral tests

- *Rotarod test.* Treated and untreated *Ube3a*$^{m-/p+}$ and wt mice (30/group) were tested, every 28 days, for locomotor disability with a Rotarod test by the same operator. Analyses started from 7 to 23 weeks of age for (n = 30/experimental group). We used the accelerating Rotarod apparatus (Ugo Basile 7650 model). Once the animals were positioned on the rotating bar, time was started and the rod was accelerated at a constant rate of 0.3 rpm/s from 3 rpm to 30 rpm for 5-min. The time (seconds) at which the animal fell from the bar was recorded. Three trials were run for each animal, with a 5-min rest between them, and the longest retention time was recorded. The mean latency to fall during the session was calculated and used in subsequent analysis.

- The *Open Field Test (OF)* was used to examine general spontaneous locomotion, as well as exploration, and the relative level of anxiety by exposing mice to a novel and an open space (Crawley, 1999; Seibenhener and Wooten, 2015; Walsh and Cummins, 1976).

We used a grey OF box (40 × 40 × 40 cm) with the floor divided into 25 (8 × 8 cm) squares. Animals were placed in the center of the arena, considered as a 'starting point', and their behavior was tracked with the activity monitoring system (Ethovision system) for 5 min. This short time was chosen to avoid further stress to mutant mice (30/group). The parameters analyzed as measures of spontaneous locomotor activity, exploratory activity and state of anxiety were: time spent in the inner zone (the nine central squares) and in the periphery of the arena (the sixteen peripheral squares), the number of crossings between the center and the periphery, the overall distance travelled, the velocity and the hypermobility.

- The *novel-object recognition test (NORT)* is a memory test based on spontaneous animal behavior without the need for stressful elements such as food or water deprivation or foot-shock (Antunes and Biala, 2012; Clarke et al., 2010). The NORT was conducted in an open-field arena (40 × 40 × 40 cm) with the floor divided into 25 squares by black lines; three stimulus objects of similar size were used: a black plastic cylinder (4 × 5 cm), a glass vial with a white cup (3 × 6 cm), and a metal cube (3 × 5 cm). The first phase of the NORT is the habituation trial in the Open Field Test, during which the animals were placed in the empty arena for 5 min. The next day, mice were placed again in the same arena containing two identical objects (familiarization phase/second phase). The objects were randomly selected to avoid bias among animals and between groups. Objects and positions were counterbalanced across experiments and behavioral trials. Exploration was recorded with the activity monitoring system (Ethovision system) in a 10-min trial. Sniffing, touching, and stretching the head toward the object were scored as object investigation. In the Novel object phase (phase 3), 24 h later, mice were placed again in the arena containing two objects: one already presented during the familiarization phase (familiar object) and a new different one (novel object). The time spent exploring the two objects was recorded for 10 min.

Results were expressed as a discrimination index (DI) (seconds spent on novel - seconds spent on familiar)/(total time spent on objects). Animals with no cognitive impairment spent longer investigating the novel object, giving a higher DI. We used 30 animals for each

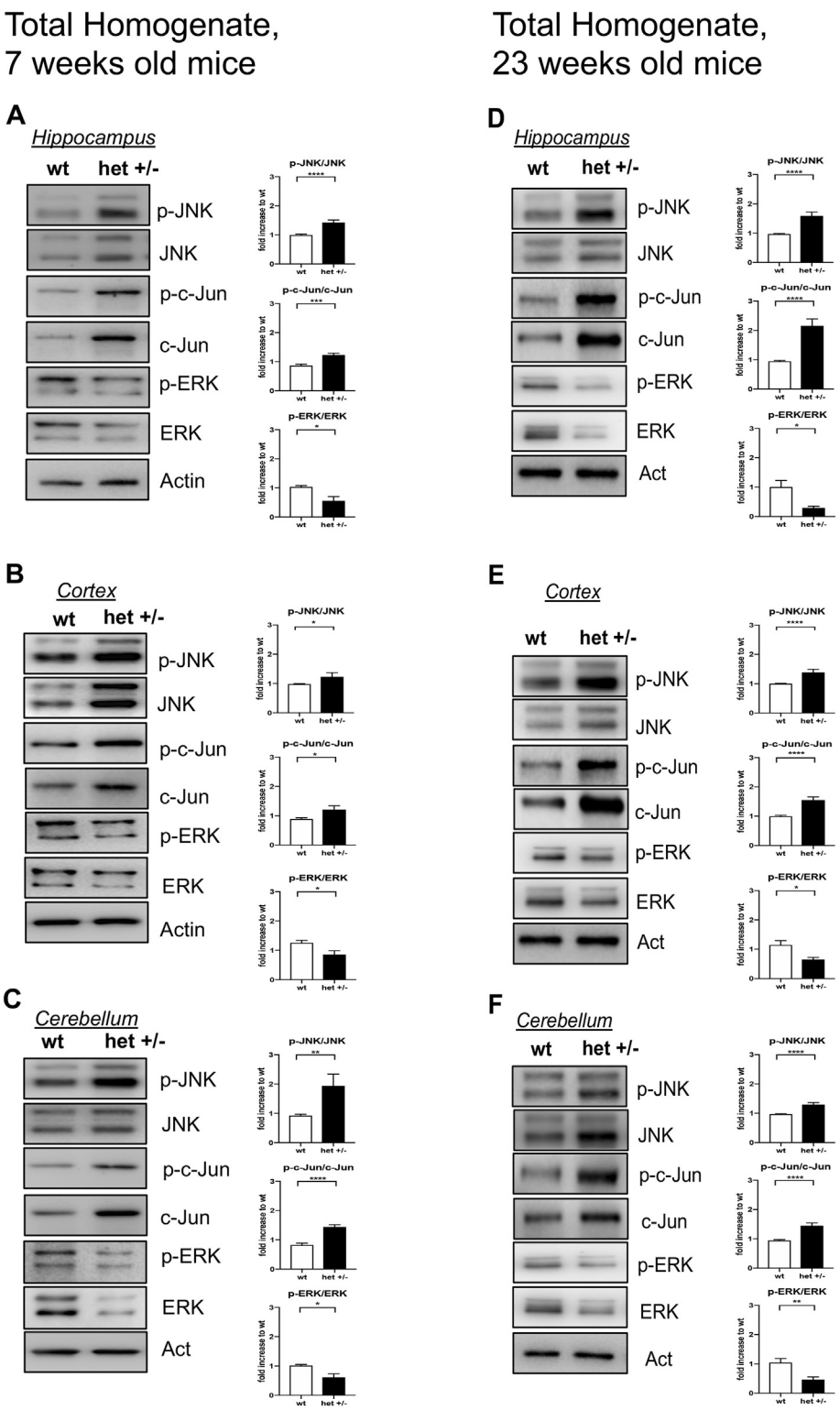

Fig. 1. Changes in JNK and ERK stress signaling pathways persist in the total homogenate from 7 to 23 weeks Ube3a $^{m-/p+}$ mice. Representative western blots and relative quantifications of total homogenate of A) hippocampus, B) cortex, C) cerebellum of 7 weeks old mice and D), E), F) of 23 weeks old mice show higher level of p-JNK/JNK, p-c-Jun/c-Jun ratios and lower p-ERK/ERK ratio in Ube3a $^{m-/p+}$ vs wt mice. Genotypes are compared using *t*-tests. Statistical significance: $*p < .05$, $**p < .01$, $***p < .001$, $****p < .0001$. Data are mean ± SEM.

experimental group.

2.4. Biochemical analysis: Subcellular fractionation (TIF)

For biochemical analysis, at the end of behavioral tests, mice were euthanized by cervical dislocation (Angus et al., 2008; Carbone et al., 2012). Brains were removed and specific areas (cortex, hippocampus and cerebellum) were dissected and stored at −80 °C until sample processing. Subcellular fractionation was as reported in the literature (Gardoni et al., 1998), with minor modifications, for cortex,

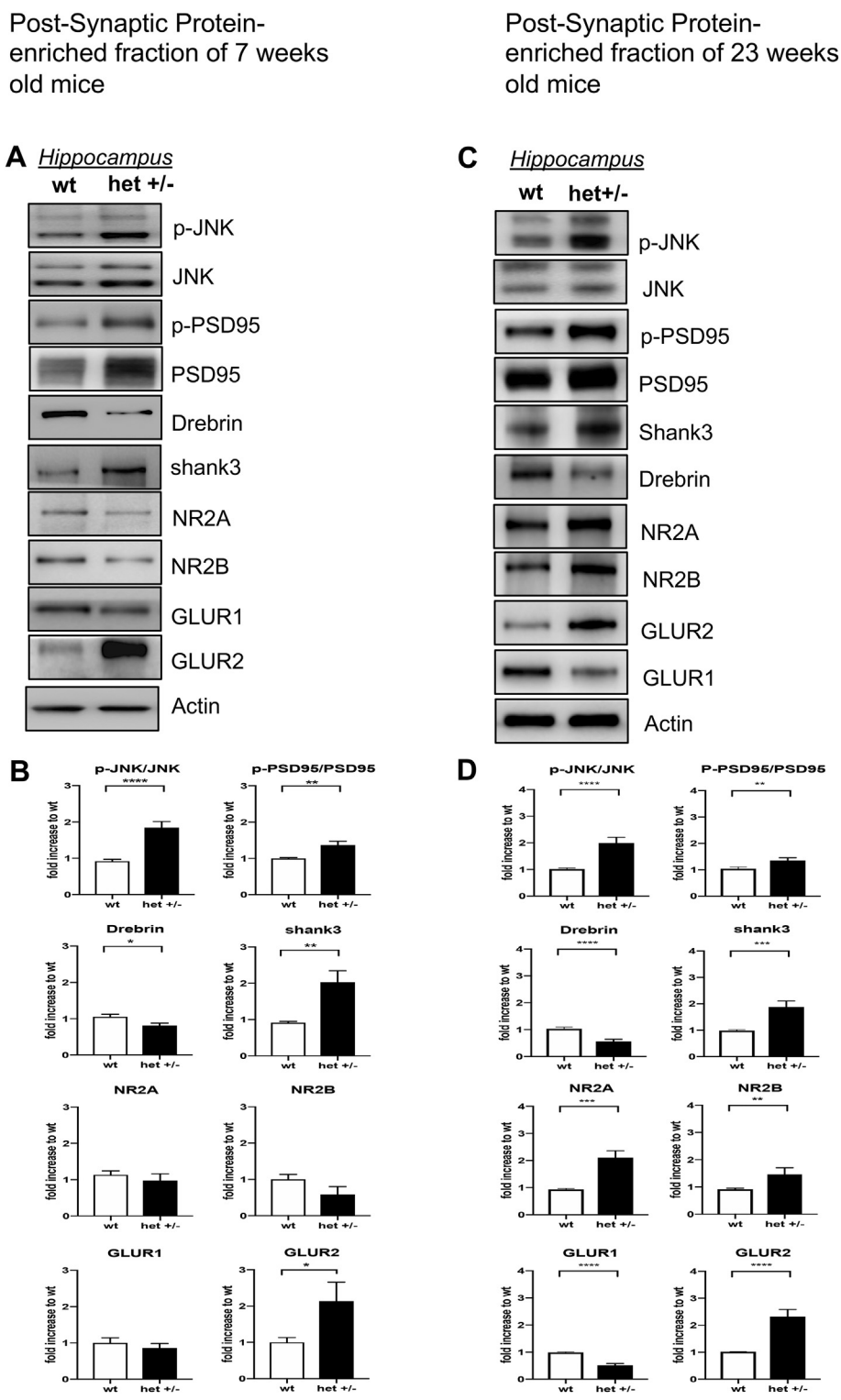

Fig. 2. Changes in JNK activation in the post-synaptic elements in the hippocampus of Ube3a $^{m-/p+}$ A) Representative western blots and B) relative quantifications showed JNK activation followed by changes in biochemical marker levels in 7 weeks-old mice. The p-PSD95/PSD95 ratio, Shank3 and GLUR2 levels are higher in Ube3a $^{m-/p+}$ mice than wt, while Drebrin level is lower. NR2A, NR2B and GLUR1 level do not differ in Ube3a $^{m-/p+}$ and wt mice. C) Representative western blots and D) relative quantifications showed JNK hyper-activation in the hippocampus TIF fraction of 23 weeks-old Ube3a $^{m-/p+}$ mice compared to wt mice. p-PSD95/PSD95 ratio, Shank3, NMDA-receptors and GLUR2 levels are higher in Ube3a $^{m-/p+}$ mice than wt, while Drebrin and GLUR1 levels are lower in Ube3a $^{m-/p+}$ mice than wt. Genotypes are compared using *t*-tests. Statistical significance:: $*p < .05$, $**p < .01$, *** p < .001, $****p < .0001$. Data are mean ± SEM.

hippocampus and cerebellum from *Ube3a*$^{m-/p+}$ and wt treated and untreated mice. Briefly, tissue was homogenized with a glass-glass Potter apparatus in 0.32 M ice-cold sucrose buffer containing the following concentrations (in mM): 1 HEPES, 1 MgCl2, 1 EDTA, 1 NaHCO3, and 0.1 PMSF, at pH 7.4, with a complete set of protease inhibitors (Complete; Roche Diagnostics, Basel, Switzerland) and phosphatase inhibitors (Sigma, St. Louis, MO). Samples were centrifuged at 1000 ×*g* for 10 min. The supernatant (S1) was then centrifuged at 3000 ×*g* for 15 min to obtain a crude membrane fraction (P2 fraction). The pellet was dissolved in buffer containing 75 mM KCl and 1% Triton X-100 plus protease and phosphatase inhibitors and centrifuged at 100,000 ×*g* for 1 h. The supernatant was stored and referred to as TSF (S4). The final pellet (P4), referred to as TIF, was homogenized in a glass Potter apparatus in 20 mM HEPES with a complete set of protease and phosphatase inhibitors and stored at −80 °C until processing.

2.5. Western blot

Protein concentrations were quantified using the Bradford Assay (Bio-Rad Protein Assay 500-0006, Munchen, Germany): 5 μg of TIF

extracted proteins and 10 μg of total homogenates were separated by 10% SDS polyacrylamide gel electrophoresis. PVDF membranes were blocked in Tris-buffered saline (5% no-fat milk powder, 0.1% Tween 20), (1 h, room temperature). Primary antibodies were diluted in the same buffer (incubation overnight, 4 °C) using anti-p-ERK (1:1000, St. Cruz), anti-ERK (1:1000, St. Cruz) anti-p-JNKs (1:1000, Cell Signaling); anti-JNKs (1:1000, Cell Signaling); anti-p-c-Jun (1:1000, Cell Signaling); anti-c-Jun (1:1000, Cell Signaling); anti-NMDA Receptor 2A GluN2A (1:2000, Gibco-Invitrogen); anti-NMDA Receptor 2B GluN2B (1:2000, Gibco-Invitrogen); anti-Glutamate Receptor 1 (AMPA subtype) GluA1 (1:1000, Millipore); anti-Glutamate Receptor 2 (AMPA subtype) GluA2 (1:1000, Millipore), anti-post-synaptic density protein 95 PSD95 (1:2000, Cayman Chemical Company), anti-p-PSD95 (1:2000, Cayman Chemical Company), anti-Actin (1:5000, Millipore), anti-Drebrin (1:1000, Cell Signaling), anti-Shank3 (1:1000, Cell Signaling). Blots were developed using horseradish peroxidase-conjugated secondary antibodies (Santa Cruz Biotechnology) and the ECL chemiluminescence system (Bio-Rad). Western blots were quantified by densitometry using ImageLab, software (Bio-Rad).

2.6. Statistical analysis

Statistical analysis was done with the Graph Pad Prism 6 program. Behavioral and biochemical parameters were analyzed using a *t*-test or Two-way ANOVA, followed by Tukey's post hoc test. Data were expressed as mean ± SEM with statistical significance $p < .05$.

3. Results

3.1. *Ube3a*$^{m-/p+}$ mice present changes in JNK and ERK signaling pathways alterations at 7 and 23 weeks of age

To investigate whether mutated-UBE3A regulates the activity of JNK and ERK kinases, we calculated the p-JNK/JNK, p-c-Jun/c-Jun and p-ERK/ERK ratios in the total homogenate of cortex, hippocampus and cerebellum of 7- and 23-week-old mice.

At 7 weeks, p-c-Jun/c-Jun and p-JNK/JNK ratios were significantly higher in *Ube3a*$^{m-/p+}$ than in age-matched wt mice (Fig. 1A–C). In *Ube3a*$^{m-/p+}$ mice the p-c-Jun/c-Jun ratio was 30% higher in the hippocampus ($p < .001$, Fig. 1A), 27% in the cortex ($p < .05$, Fig. 1B), and 43% in the cerebellum ($p < .0001$, Fig. 1C) than in wt mice. Thus, JNK activity was significantly higher in *Ube3a*$^{m-/p+}$ mice than in age-matched wt mice, while p-ERK/ERK ratio was 46% lower in the hippocampus ($p < .05$, Fig. 1A), 32% in the cortex ($p < .05$, Fig. 1B) and 40% in the cerebellum ($p < .05$, Fig. 1C) than in wt mice.

The p-JNK/JNK, p-c-Jun/c-Jun and p-ERK/ERK ratios in the total homogenate of cortex, hippocampus and cerebellum were also measured at 23 weeks of age to determine the importance of stress signaling in the progression of *Ube3a* $^{m-/p+}$ pathology. JNK activity was significantly higher in *Ube3a* $^{m-/p+}$ mice than in age-matched wt mice (39% in the hippocampus, 27% in the cortex and 25% in the cerebellum, $p < .0001$; $p < .0001$; $p < .0001$, Fig. 1D–F).

The early stage, the JNK signaling pathway was still powerfully activated in all brain areas. These findings illustrate that JNK activation persists until 23 weeks of age at an advanced stage of the AS pathology.

3.2. *Ube3a* $^{m-/p+}$ mice show changes in PSD biochemical markers and JNK activation in the post-synaptic protein-enriched fraction at 7 weeks of age

To study *Ube3a*$^{m-/p+}$ post-synaptic elements we analyzed the molecular organization of the PSD-region isolating the post-synaptic protein-enriched fraction (TIF) of hippocampus, cortex and cerebellum.

We measured JNK activation in the post-synaptic elements, in *Ube3a* $^{m-/p+}$ hippocampus compared to wt mice. The P-JNK/JNK ratio was significantly higher in *Ube3a*$^{m-/p+}$ (50%, $p < .0001$, Fig. 2A–B) than wt mice. We also measured the p-PSD95/PSD95 ratio (Fig. 2A–B), using a p-PSD95 antibody that recognizes the specific JNK phosphorylation site. The ratio was significantly higher in *Ube3a*$^{m-/p+}$ (27%) than wt mice ($p < .01$, Fig. 2A–B).

In addition, to analyze the molecular organization of *Ube3a* $^{m-/p+}$ post-synaptic elements better, we quantified other PSD markers: Shank3, a scaffold protein strongly implicated in autism, Drebrin, a marker of mature spines and AMPA and NMDA receptors. Shank3 and GLUR2 levels were significantly higher in *Ube3a*$^{m-/p+}$ (55% and 53%; $p < .01$, $p < .05$, Fig. 2A–B), while Drebrin was 23% lower than in wt mice ($p < .05$, Fig. 2A–B). NR2A, NR2B and GLUR1 levels showed no significantly change in *Ube3a* $^{m-/p+}$ (Fig. 2A–B). These results indicate abnormal protein expression and/or organization of the PSD region in *Ube3a*$^{m-/p+}$ mice.

We analyzed JNK activation at the post-synaptic elements in the cortex as well. The p-JNK/JNK ratio was significantly higher (45%) in *Ube3a* $^{m-/p+}$ than wt mice ($p < 0{,}0001$, Fig. S1A), indicating JNK activation in the post-synaptic protein-enriched fraction. The p-PSD95/PSD95 ratio was significantly higher in *Ube3a*$^{m-/p+}$ (28%) than wt mice ($p < .0001$, Fig. S1A). In *Ube3a*$^{m-/p+}$ the Shank3 level was 51% higher and Drebrin 43% lower than in wt mice ($p < .001$ and $p < .01$, Fig. S1A). In addition, *N*-methyl-D-aspartate receptor 2A NR2A (45%) and AMPA receptor subunits GLUR1 (30%) were significantly lower in *Ube3a*$^{m-/p+}$ than in wt mice ($p < .05$, $p < .05$, Fig. S1A), while NR2B and GLUR2 levels showed no change (Fig. S1A).

Finally, we also examined JNK activation in the post-synaptic elements in the cerebellum, in *Ube3a*$^{m-/p+}$ compared to wt mice. At this stage there is only a tendency for an increase of p-JNK/JNK ratio in *Ube3a*$^{m-/p+}$ compared to wt, meaning that JNK activation is not as strong as in the other areas. The p-PSD95/PSD95 ratio (29%) and Shank3 level (46%) were significantly higher in *Ube3a*$^{m-/p+}$ than wt ($p < .05$, $p < .001$, Fig. S1B) while Drebrin (59%), NR2A (70%), NR2B (71%), GLUR1 (41%) and GLUR2 (58%) levels were significantly lower ($p < .001$, $p < .05$, $p < .01$, $p < .05$, $p < .01$, Fig. S1B).

3.3. *Ube3a* $^{m-/p+}$ mice present behavioral impairments at 7 weeks of age

Ube3a $^{m-/p+}$ TIF fraction showed significant biomarker changes in the 3 different brain areas analyzed. In order to correlate *Ube3a*$^{m-/p+}$ synaptic dysfunctions to both cognitive and locomotor defects we examined cognitive impairment with the Novel Object Recognition Test (NORT) and locomotor defects with the Open Field and Rotarod tests.

In the NORT, *Ube3a*$^{m-/p+}$ mice had a significantly lower discrimination index (DI) (96%) than aged-matched wt mice ($p < 0{,}05$, Fig. 3A). At 7 weeks of age the *Ube3a* $^{m-/p+}$ DI was 0.009422, and the wt DI 0.2712. These data confirm the severe cognitive impairment in *Ube3a* $^{m-/p+}$ mice already at 7 weeks of age.

To investigate spontaneous locomotor and exploratory activity in *Ube3a*$^{m-/p+}$ we ran the Open Field test on the same animals. *Ube3a*$^{m-/p+}$ mice had significantly lower velocity (15%) and shorter distance moved (14%) than aged-matched wt mice ($p < .05$, Fig. 3B). The total number of crossing was significantly lower too (21%) in *Ube3a*$^{m-/p+}$ than wt mice ($p < .05$, Fig. 3B). These data confirm locomotor impairments in *Ube3a*$^{m-/p+}$ mice.

Exploratory activity was measured as the time spent in the inner zone and the outer zone (Fig. 3B): *Ube3a* $^{m-/p+}$ mice spent more time (9%, $p < .01$) in the outer zone of the arena but the time spent in the inner zone was no significantly different from aged-matched wt mice. In addition, *Ube3a* $^{m-/p+}$ mice also had an increased hypermobility state (95%, $p < .01$, Fig. 3B) compared to age-matched wt mice. To summarize, *Ube3a*$^{m-/p+}$ mice showed a mild exploratory impairment at 7 weeks compared to wt mice but had a severe hypermobility symptom.

The *Ube3a*$^{m-/p+}$ locomotor impairment was then characterized in the Rotarod test. *Ube3a*$^{m-/p+}$ had a shorter (17%) latency to fall on the accelerated rod than to aged-matched wt mice, with significantly reduced locomotor ability at 7 weeks of age ($p < .05$, Fig. 3C).

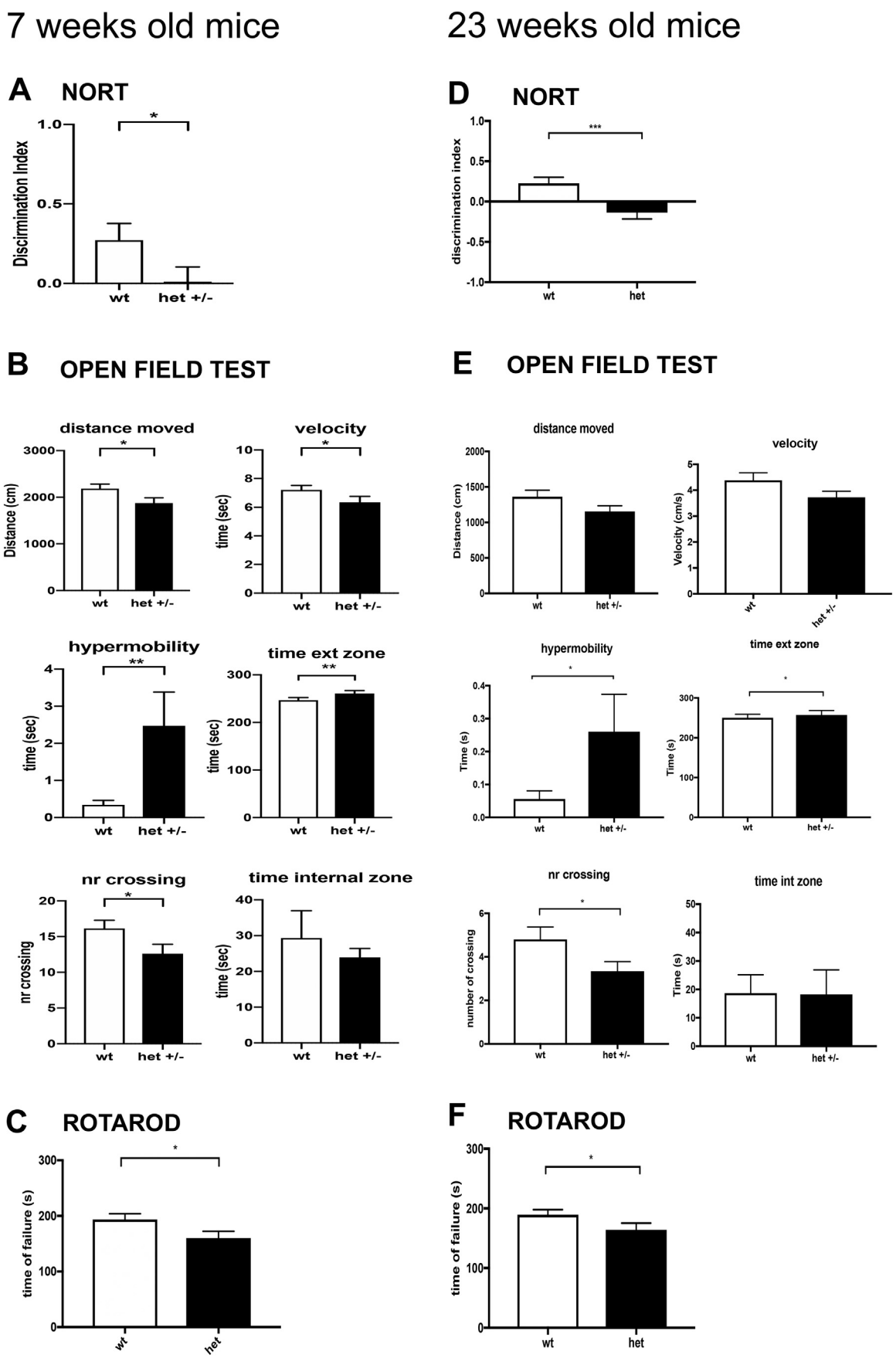

(caption on next page)

Fig. 3. Ube3a $^{m-/p+}$ mice show severe cognitive impairment and mild locomotor and exploratory defects. 7 weeks-old Ube3a $^{m-/p+}$ mice give a lower DI in the NORT than aged-matched wt mice (A). The Open Field Test (B) shows the shorter distance moved, velocity and smaller number of crossing in Ube3a $^{m-/p+}$ mice than wt. Ube3a $^{m-/p+}$ mice also had increased hypermobility and spent more time in the outer zone of the arena and less time in the inner zone (not significant). Ube3a $^{m-/p+}$ mice also had a shorter time to failure in the Rotarod test compared to wt mice (C).
23 weeks-old Ube3a $^{m-/p+}$ mice show cognitive impairment indicated by a smaller DI in the NORT compared to aged-matched wt mice (D). The Open Field test (E) show no significant differences in distance, velocity, and time spent in the inner zone between wt and Ube3a $^{m-/p+}$ mice. Ube3a $^{m-/p+}$ mice had fewer crossings between the inner and outer zones of the arena and spent more time in the outer zone compared to wt mice. Ube3a $^{m-/p+}$ mice were also more hypermobile than wt. In the Rotarod test (F) Ube3a $^{m-/p+}$ mice had a shorten latency to fall on the rod than aged-matched wt mice. Genotypes were compared using t-tests. Statistical significance: *p < .05, **p < .01, ***p < .001. Data are mean ± SEM.

These results suggest that *Ube3a*$^{m-/p+}$ mice at 7 weeks of age present an important cognitive impairment while the locomotor defects seem milder than in aged-matched wt mice.

3.4. Ube3a $^{m-/p+}$ mice present changes in PSD biochemical markers and a persistent JNK activation in the post-synaptic element at 23 weeks of age

We characterized the synaptic dysfunction of *Ube3a*$^{m-/p+}$ mice at 23 weeks of age. Here we presented only the hippocampal results because the data concerning other areas are in line with hippocampal findings (in supplementary Figs. S2A–B). The post-synaptic protein-enriched fraction still presented JNK activation, and in fact the p-JNK/JNK ratio was 49% higher in *Ube3a*$^{m-/p+}$ than wt ($p < .0001$, Fig. 2C–D). The p-PSD95/PSD95 ratio (22%), Shank3 (47%), NR2A (55%), NR2B (25%) and GLUR2 (56%) levels were significantly higher in *Ube3a*$^{m-/p+}$ than wt mice ($p < .01$, $p < .001$, $p < .001$, $p < .01$, $p < .0001$, Fig. 2C–D) while Drebrin (45%) and GLUR1 (47%) levels were lower than in wt mice ($p < .0001$, Fig. 2C–D).

3.5. Ube3a $^{m-/p+}$ mice present behavioral impairments at 23 weeks of age

Cognitive and locomotor defects in *Ube3a*$^{m-/p+}$ mice were examined at 23 weeks of age. In the NORT, *Ube3a*$^{m-/p+}$ mice had a significantly lower DI than aged-matched wt mice ($p < .001$, Fig. 3D). Wt mice had a DI of 0.272, and *Ube3a* $^{m-/p+}$ DI had −0.1352 while at 7 weeks it was 0.009422. These data indicate that *Ube3a*$^{m-/p+}$ cognitive impairments get worse with the progression of the AS pathology.

The Open Field test was run at 23 weeks to assess the spontaneous locomotor and exploratory activity in *Ube3a*$^{m-/p+}$ and wt mice. Surprisingly, *Ube3a*$^{m-/p+}$ mice did not significantly differ in velocity and distance moved from aged-matched wt mice (Fig. 3E), indicating no genotypic differences. However, at 23 weeks the total number of crossings was significantly smaller (30%) in *Ube3a* $^{m-/p+}$ ($p < .05$, Fig. 3E).

As regards exploratory activity, the time spent by *Ube3a*$^{m-/p+}$ mice in the inner zone did not significantly differ from the time spent by aged-matched wt mice (Fig. 3E), while the time spent in the outer zone was higher ($p < .05$, Fig. 3E).

Finally, *Ube3a*$^{m-/p+}$ mice still presented an increased hypermobility (78%, $p < .05$, Fig. 3E) compared to age-matched wt mice. The *Ube3a*$^{m-/p+}$ mice locomotor impairment at 23 weeks was not significantly different from wt mice, although there were fewer crossings and the evident hypermobility symptoms persisted at this stage of the AS pathology of mice.

Ube3a$^{m-/p+}$ locomotor impairment was further characterized in the Rotarod test. At 23 weeks *Ube3a*$^{m-/p+}$ mice still had a shorter latency time (13%) on the rod than aged-matched wt mice, with a significant decrease of locomotor ability at 23 weeks of age ($p < .05$, Fig. 3F).

3.6. Specific D-JNKI1 treatment prevents JNK signaling activation in 23 weeks old Ube3a $^{m-/p+}$ mice

To determine the role of JNK in *Ube3a*$^{m-/p+}$ pathology we used the specific JNK inhibitor peptide, D-JNKI1, injected intraperitoneally every 4 weeks from 7 to 23 weeks of age, to inhibit JNK's action in *Ube3a*$^{m-/p+}$ mice and, as a control, in wt mice. There were four groups: 1-D-JNKI1-treated wt 2-untreated wt mice and 3-D-JNKI1-treated *Ube3a*$^{m-/p+}$ and 4-untreated *Ube3a*$^{m-/p+}$ mice.

D-JNKI1's inhibitory effect is measured as a reduction of p-JNK/JNK and p-c-Jun/c-Jun ratios in the cortex, hippocampus and cerebellum in vivo (Borsello et al., 2003). In addition, to assess the compensatory effect we also calculated the p-ERK/ERK ratio, as previously observed.

D-JNKI1 powerfully prevented JNK and c-Jun phosphorylation in the hippocampus (44%, $p < .0001$; 51%, $p < .01$, Fig. 4A), cortex (55%, $p < .0001$; 30%, $p < .001$% Fig. S3A), and cerebellum (26%, $p < .001$; 40%, $p < .0001$ Fig. S4A) in the treated compared to untreated *Ube3a*$^{m-/p+}$ mice, but had no significant effect in wt mice.

As expected, ERK phosphorylation increased of 79% in the hippocampus ($p < .001$, Fig. 4A), 71% in the cortex ($p < .001$, Fig. S3A), and 72% in the cerebellum ($p < .0001$, Fig. S4A) in D-JNKI1-treated *Ube3a* $^{m-/p+}$ mice compared to untreated mice, while the treatment had no effects in wt mice, confirming the absence of major side effects of the peptide in control mice. These data confirm the efficacy and specificity of D-JNKI1 in the cortex, hippocampus and cerebellum in vivo and suggests there are no major side effects in control conditions.

3.7. D-JNKI1 normalizes biochemical post-synaptic protein-enriched fraction changes in 23 weeks old Ube3a$^{m-/p+}$ mice

D-JNKI1 normalized the biochemical changes in the post-synaptic protein-enriched fraction of the hippocampus, cortex and cerebellum in *Ube3a*$^{m-/p+}$ mice. In the hippocampus D-JNKI1 reduced the p-JNK/JNK and p-PSD95/PSD95 ratios (to 49% and 26%), ($p < .0001$, $p < .05$, Fig. 4B) compared to untreated *Ube3a*$^{m-/p+}$ mice. Shank3 and Drebrin levels were both regularized to control levels. D-JNKI1 also normalized the levels of NR2B (72%, $p < .01$, Fig. 4B), GLUR1 33% ($p < .05$, Fig. 4B) and GLUR2 40% ($p < .01$, Fig. 4B) compared to untreated *Ube3a*$^{m-/p+}$ mice, while there was no effect on NR2A. As regards D-JNKI1 inhibition on wt mice, there were no significant changes in PSD markers, suggesting no major toxic effects.

D-JNKI1 also rescued the biochemical changes observed in the cortex post-synaptic protein-enriched fraction of 23-week old *Ube3a*$^{m-/p+}$ mice. Briefly, the treatment powerfully reduced (58%) the p-JNK/JNK ratio in the post-synaptic elements of treated *Ube3a*$^{m-/p+}$ compared to untreated mice ($p < .001$, Fig. S3B). The p-PSD95/PSD95 ratio was lower (35%, $p < .01$, Fig. S3B) in treated *Ube3a* $^{m-/p+}$ compared to untreated *Ube3a*$^{m-/p+}$ mice (Fig. S3B); Shank3 was lower as well (70%, $p < .0001$, Fig. S3B), while Drebrin did not significantly change. D-JNKI1 restored NMDA and AMPA receptor levels. NR2A decreased 64% ($p < .0001$, Fig. S3B), NR2B 49% ($p < .01$, Fig. S3B), GLUR1 39% ($p < .01$, Fig. S3B) and GLUR2 61% ($p < .0001$, Fig. S3B) in treated compared to untreated *Ube3a*$^{m-/p+}$ mice. D-JNKI1 normalized the biochemical marker levels of *Ube3a*$^{m-/p+}$ treated mice and had no significant effect in wt mice.

Finally, D-JNKI1 at 23 week normalized biochemical marker levels in the cerebellum of *Ube3a*$^{m-/p+}$ mice. In the cerebellum, like in the others brain regions, D-JNKI1 reduced the p-JNK/JNK (38%) and p-PSD95/PSD95 (54%) ratios in the post-synaptic protein-enriched fraction compared to untreated *Ube3a*$^{m-/p+}$ mice ($p < .001$, $p < .0001$, Fig. S4B). Shank3 and Drebrin levels were both regularized, while the treatment raised the NMDA (70%, $p < 0,05$ for NR2B, not significant

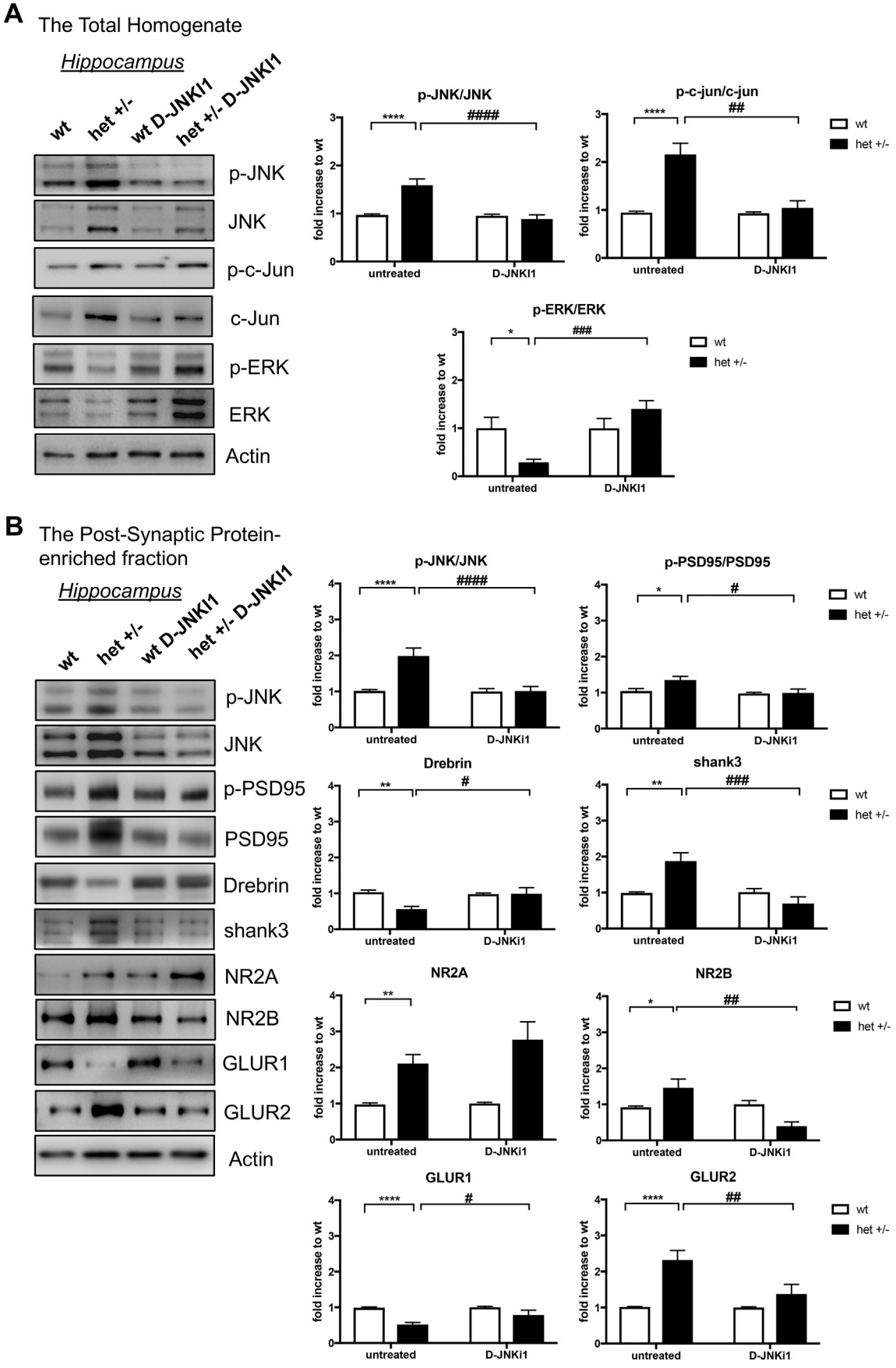

(caption on next page)

Fig. 4. D-JNKI1 chronic treatment reduced JNK activation in the hippocampus total homogenate and in the TIF fraction of 23 weeks old Ube3a $^{m-/p+}$ mice. (A) Representative western blots and relative quantifications show the higher p-JNK/JNK and p-c-Jun/c-Jun ratios in the Hippocampus total homogenate of 23 week-old Ube3a$^{m-/p+}$ mice, while the p-ERK/ERK ratio is lower. D-JNKI1 blocks the JNK signaling pathway activation and potentiates ERK signaling. The treatment had no changes in wt mice. (B) Representative western blots and quantifications show JNK activation in the hippocampus TIF fraction of Ube3a$^{m-/p+}$ mice at 23 week of age with higher levels of p-PSD95/PSD95, Shank3, NR2A, NR2B and GLUR2 then in wt mice. On the contrary, Drebrin and GLUR1 levels are reduced in Ube3a$^{m-/p+}$ mice to age-matched wt. D-JNKI1 reduced JNK activation, the p-PSD95/PSD95 ratio, Shank3 and NR2B levels but raised Drebrin, GLUR1 and NR2A (not significant) levels in treated compared to untreated Ube3a$^{m-/p+}$ mice. The treatment did not cause any changes in wt. Significance differences from control *$p < .05$, **$p < .01$, ****$p < .0001$; D-JNKI1 treated vs untreated: #$p < .05$, ##$p < .01$, ### $p < .001$, #### $p < .0001$. Two-way ANOVA, Tukey's post-hoc test. Data are mean ± SEM.

for NR2A, Fig. S4B) and AMPA receptor levels (GLUR1 62%, GLUR2 38%, $p < .0001$, $p < .01$ Fig. S4B) compared to untreated mice. No significant effects were seen on treated wt mice (Fig. S4B).

These data indicate that the D-JNKI1 normalizes biochemical post-synaptic protein-enriched fraction alterations in vivo in the three brain areas studied.

3.8. D-JNKI1 rescues cognitive impairments but not locomotor defects

To evaluate the potential neuroprotective effect of D-JNKI1 on cognitive impairment we investigated untreated and treated *Ube3a*$^{m-/p+}$ and wt mice in the NORT during chronic treatment at the indicated times (from 7 to 23 weeks). The *Ube3a*$^{m-/p+}$ DI was always lower than aged-matched wt mice, and the genotypic difference increased with the severity of the AS-pathology as expected (159% $p < .0001$, Fig. 5A1-A2). At 23 week the *Ube3a*$^{m-/p+}$ had a significantly lower DI than aged-matched wt mice. D-JNKI1 had no effect in wt in fact the two curves (continue and dotted) overlap (Fig. 5A4). However, with the chronic D-JNKI1 treatment we found a significant difference between treated *Ube3a*$^{m-/p+}$ and untreated mice; their performances were significantly better (144%) at 23 weeks of age, reaching an average DI of 0.31 compared to untreated *Ube3a*$^{m-/p+}$ (average DI of −0.1352, Fig. 5A3). D-JNKI1 rescued the cognitive impairment in *Ube3a*$^{m-/p+}$ mice.

D-JNKI1's effect on the locomotor defect was investigated in the Rotarod test because, at 23 weeks, the genotypic differences between *Ube3a*$^{m-/p+}$ and wt mice were not significantly different in the Open Field test (see Fig. 3E) while in the Rotarod the differences remained significant. In the four groups previously described (untreated and treated wt and *Ube3a*$^{m-/p+}$ mice) from 7 to 23 weeks of age, there was an overall genotypic difference between wt and *Ube3a*$^{m-/p+}$ mice ($p < .0001$, Fig. 5B1–B2). At the last time point, *Ube3a*$^{m-/p+}$ mice spent 13% less time on the rotating bar than wt mice Fig. 5B2). We found no significant effect in treated *Ube3a*$^{m-/p+}$ and untreated *Ube3a*$^{m-/p+}$ (Fig. 5B3). D-JNKI1 had no effect in treated vs untreated wt mice (continue vs dotted lines) (Fig. 5B4). In conclusion chronic D-JNKI1 treatment had no positive effect on locomotor impairments.

4. Discussion

The *Ube3a* maternal deficient mouse model recapitulates different pathological symptoms associated with AS syndrome including impaired hippocampal long-term potentiation and reduced dendritic spine density, together with cognitive and motor deficits and inducible seizures (Dindot et al., 2008; Jiang et al., 1998; Sato and Stryker, 2010; Weeber et al., 2003; Yashiro et al., 2009).

Although mutations in the UBE3A gene result in AS pathology, little is known yet about the role of UBE3A in the nervous system and/or how UBE3A mutation/loss induces neuronal degeneration, with consequent cognitive and locomotor impairments. The cellular mechanisms of the downstream effects of UBE3A loss in neurons are still lack, thus there are still no effective treatments.

This study sheds new light on the neuronal alterations caused by UBE3A mutation/loss of function and provides the first proof of principle of an important downstream JNK role in *Ube3a*$^{m-/p+}$ pathology.

We report here that *Ube3a*$^{m-/p+}$ mice presented high JNK activation both in the soma and in postsynaptic elements. The JNK pathway is activated in the early stage of AS pathology, at 7 weeks of age (a stage comparable to adolescence), and still persists in adulthood (23 weeks), suggesting an important function of this stress pathway in AS. The high JNK activation in the brain of *Ube3a*$^{m-/p+}$ is balanced, as often happens, by a drop in ERK phosphorylation.

We also found that *Ube3a*$^{m-/p+}$ mice had changes in the PSD marker levels in the post-synaptic protein-enriched fraction, indicating more immature spines. These generalized alterations of the PSD markers in cortex, cerebellum and hippocampus, caused by the loss of UBE3A, are in line with the reduced dendritic spine density observed in AS patients (Jay et al., 1991) and AS mouse models (Cooper et al., 2003; Dindot et al., 2008; Sato and Stryker, 2010; Wallace et al., 2012; Yashiro et al., 2009).

With the PSD marker levels alterations in the post-synaptic element we also found powerful JNK activation, at 7 and at 23 weeks of age, suggesting that JNK pathway is involved in synaptic dysfunction in AS, as reported in other brain disease models (Buccarello et al., 2018; Sclip et al., 2014; Sclip et al., 2013; Sclip et al., 2011).

The synaptic defects in this mouse model is related with behavioral impairments: *Ube3a* $^{m-/p+}$ mice had cognitive deficits starting in the first phase of AS pathology (7 weeks), which then increased with age (23 weeks). After chronic treatment with D-JNKI1 the treated-*Ube3a* $^{m-/p+}$ D.I. was 0.31, while the untreated *Ube3a*$^{m-/p+}$ DI was −0.1352, D-JNKI1 leading the *Ube3a*$^{m-/p+}$ performance closer to control level (wt DI was 0.272).

On the other hand, the *Ube3a*$^{m-/p+}$ mice show also a locomotor impairment, however, these deficits did not increase with age (from 7 to 23 weeks) like the cognitive one, and instead remained constant in the Rotarod test. The OF test detected locomotor impairments only at 7 weeks of age, while at 23 weeks of age there was no genotypic difference between wt and *Ube3a*$^{m-/p}$ mice. However, despite this, *Ube3a*$^{m-/p}$ mice presented synaptic alterations in both the early and late stages of the pathology, suggesting that their motor defects are not highlighted by these tests, more sensitive and accurate behavioral tests are needed.

In neurodegenerative processes, JNK has a double function: it phosphorylates the transcription factor c-Jun in the nucleus, thus activating the neuronal death program, and phosphorylates PSD95, alterating PSD marker levels (Sclip et al., 2011, 2013) as well as the morphological structure of the postsynaptic element (Sclip et al., 2014).

Ube3a $^{m-/p+}$ mice had higher levels of p-c-Jun in the brain than wt mice, indicating the activation of neuronal death pathway. These mice also showed synaptic dysfunction, as demonstrated by changes in the PSD biomarkers of the post-synaptic protein-enriched fraction, together with JNK activation, confirmed by the specific increase of the p-PSD95/PSD95 ratio in the post-synaptic elements. This is the first neurodegenerative event that can progress in neuronal death.

This is the first indication that, in the brain, the loss of E3 ubiquitin ligase UBE3A activates the JNK stress signaling pathway. However, to determine the importance of JNK's role in this AS model, we applied a chronic, specific inhibition of JNK in *Ube3a*$^{m-/p+}$ mice to see whether JNK inhibition blocked AS pathology and could offer a new pharmacological opportunity against AS.

D-JNKI1 treatment in *Ube3a*$^{m-/p+}$ mice, starting at 7 weeks of age and ending at 23 weeks of age, inhibited c-Jun phosphorylation in

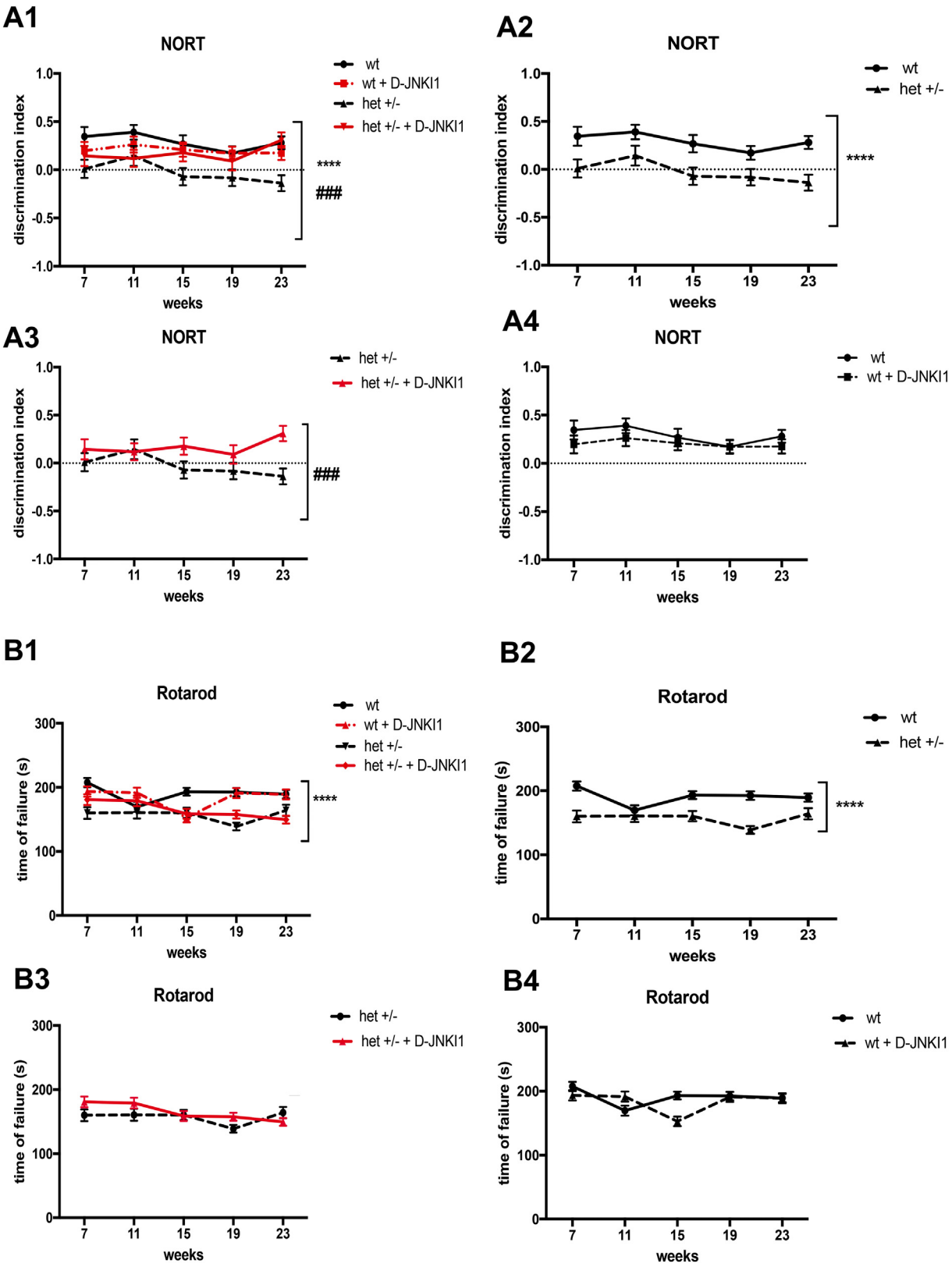

Fig. 5. D-JNKI1 prevents cognitive impairments in Ube3a$^{m-/p+}$ mice in the Novel object recognition test but not locomotor impairments. A1) Cognitive performances over time in treated and untreated Ube3a$^{m-/p+}$ and wt mice. A2) The discrimination index was significantly lower in Ube3a$^{m-/p+}$ mice (red line) than wt (black line). A3) DJNKI1 treatment restored the cognitive impairment in treated Ube3a$^{m-/p+}$ (red line) mice compared to untreated Ube3a$^{m-/p+}$ mice (black line) at 23 weeks of age, with no significant effect on treated wt (dotted black line) compared to untreated wt mice (continuous black line) (A4). From 7 to 23 weeks of age, in the Rotarod test, treated and untreated, Ube3a$^{m-/p+}$ mice (dotted line) showed locomotor impairment compared to wt (continuous black line) (B1-B2). However, D-JNKI1 did not induce any significant improvement in Ube3a$^{m-/p+}$ (red line) compared to untreated Ube3a$^{m-/p+}$ mice (black line) (B3) or in wt (dotted black line) compared to untreated wt (continuous black line) (B4). Statistical significance: ****p $<$ .0001, *###p* $<$ .001. Two-way ANOVA, Tukey's post-hoc test. Data are mean $\pm$ SEM.

Ube3a$^{m-/p+}$ in all the brain areas studied in vivo. Furthermore, by inhibiting JNK signaling, the p-ERK/ERK ratio increased up to wt level, as expected. It is well known that c-Jun is the elective target of JNK and, importantly, it is phosphorylated in response to many different stress stimuli. c-Jun is involved in multiple cellular processes like gene expression, apoptosis, metabolism and other critical physiological responses (Kuan et al., 1999; Yang et al., 1997).

Notably, JNK inhibition (D-JNKI1) powerfully inhibits the phosphorylation of c-Jun in the nuclei of cortical, hippocampal and cerebellar neurons, preventing their neurodegenerative pathway. In addition, the treatment also normalized the previously observed biochemical alterations in the post-synaptic protein-enriched fraction, and the p-JNK/JNK and p-PSD95/PSD95 ratios were reduced in all the brain areas.

The neuroprotection on the post-synaptic elements is paired by the NORT results: D-JNKI1 rescued *Ube3a*$^{m-/p+}$ cognitive impairments to the control level. Both the biochemical and functional findings strengthen the neuroprotection obtained with D-JNKI1, giving hope for a possible clinical application. Last but not least, D-JNKI1 treatment in wt mice did not show any significant adverse effects. The treatment also powerfully inhibits the c-jun phosphorylation in the cortex, hippocampus and cerebellum, preventing the neurodegenerative-stress pathway.

This is the first proof of concept that in the brain the E3 ubiquitin ligase UBE3A loss induces the downstream activation of the JNK stress signaling pathway. This link between UBE3A and JNK may be indirect, but is pivotal in the AS. In fact, the specific inhibition of JNK prevents c-Jun phosphorylation, rescues the spine alterations and the cognitive impairments in *Ube3a*$^{m-/p+}$ mice, tackles the pathology.

In our opinion these data provide evidences of the therapeutical utility of D-JNKI1 treatment against AS.

Funding

This work was supported by Angelman Syndrome Alliance (ASA) grant.

Declaration of Competing Interest

The authors declare no actual or potential conflicts of interest.

Acknowledgments

The authors gratefully acknowledge Dot. M. Tettamanti for the support in statistical analysis, J. Baggott that kindly edited the text. Erika Iervasi and Francesco Santarella for their advices and criticisms. A special thanks goes to the ORSA - Associazione Sindrome di Angelman that has strongly supported this project.

Appendix A. Supplementary data

Supplementary data to this article can be found online at https://doi.org/10.1016/j.nbd.2020.104812.

References

Angus, D.W., Baker, J.A., Mason, R., Martin, I.J., 2008. The potential influence of CO2, as an agent for euthanasia, on the pharmacokinetics of basic compounds in rodents. Drug Metab. Dispos. 36, 375–379. https://doi.org/10.1124/dmd.107.018879.

Antoniou, X., Borsello, T., 2010. Cell permeable peptides: a promising tool to deliver neuroprotective agents in the brain. Pharmaceuticals (Basel) 3, 379–392. https://doi.org/10.3390/ph3020379.

Antunes, M., Biala, G., 2012. The novel object recognition memory: neurobiology, test procedure, and its modifications. Cogn. Process. 13, 93–110. https://doi.org/10.1007/s10339-011-0430-z.

Auladell, C., de Lemos, L., Verdaguer, E., Ettcheto, M., Busquets, O., Lazarowski, A., Beas-Zarate, C., Olloquequi, J., Folch, J., Camins, A., 2017. Role of JNK isoforms in the kainic acid experimental model of epilepsy and neurodegeneration. Front. Biosci. (Landmark Ed.) 22, 795–814. https://doi.org/10.2741/4517.

Biggi, S., Buccarello, L., Sclip, A., Lippiello, P., Tonna, N., Rumio, C., Di Marino, D., Miniaci, M.C., Borsello, T., 2017. Evidence of presynaptic localization and function of the c-Jun N-terminal kinase. Neural Plast. 2017, 6468356. https://doi.org/10.1155/2017/6468356.

Borsello, T., Clarke, P.G.H., Hirt, L., Vercelli, A., Repici, M., Schorderet, D.F., Bogousslavsky, J., Bonny, C., 2003. A peptide inhibitor of c-Jun N-terminal kinase protects against excitotoxicity and cerebral ischemia. Nat. Med. 9, 1180–1186. https://doi.org/10.1038/nm911.

Buccarello, L., Sclip, A., Sacchi, M., Castaldo, A.M., Bertani, I., ReCecconi, A., Maestroni, S., Zerbini, G., Nucci, P., Borsello, T., 2017. The c-jun N-terminal kinase plays a key role in ocular degenerative changes in a mouse model of Alzheimer disease suggesting a correlation between ocular and brain pathologies. Oncotarget 8, 83038–83051. https://doi.org/10.18632/oncotarget.19886.

Buccarello, L., Musi, C.A., Turati, A., Borsello, T., 2018. The stress c-Jun N-terminal kinase signaling pathway activation correlates with synaptic pathology and presents a sex bias in P301L mouse model of tauopathy. Neuroscience 393, 196–205. https://doi.org/10.1016/j.neuroscience.2018.09.049.

Carbone, L., Carbone, E.T., Yi, E.M., Bauer, D.B., Lindstrom, K.A., Parker, J.M., Austin, J.A., Seo, Y., Gandhi, A.D., Wilkerson, J.D., 2012. Assessing cervical dislocation as a humane euthanasia method in mice. J. Am. Assoc. Lab. Anim. Sci. 51, 352–356.

Clarke, J.R., Cammarota, M., Gruart, A., Izquierdo, I., Delgado-García, J.M., 2010. Plastic modifications induced by object recognition memory processing. Proc. Natl. Acad. Sci. U. S. A. 107, 2652–2657. https://doi.org/10.1073/pnas.0915059107.

Coffey, E.T., 2014. Nuclear and cytosolic JNK signalling in neurons. Nat. Rev. Neurosci. 15, 285–299. https://doi.org/10.1038/nrn3729.

Colombo, A., Bastone, A., Ploia, C., Sclip, A., Salmona, M., Forloni, G., Borsello, T., 2009. JNK regulates APP cleavage and degradation in a model of Alzheimer's disease. Neurobiol. Dis. 33, 518–525. https://doi.org/10.1016/j.nbd.2008.12.014.

Cooper, B., Schneider, S., Bohl, J., Jiang, Y. Hui, Beaudet, A., Vande Pol, S., 2003. Requirement of E6AP and the features of human papillomavirus E6 necessary to support degradation of p53. Virology 306, 87–99. https://doi.org/10.1016/s0042-6822(02)00012-0.

Crawley, J.N., 1999. Behavioral phenotyping of transgenic and knockout mice: experimental design and evaluation of general health, sensory functions, motor abilities, and specific behavioral tests. Brain Res. 835, 18–26. https://doi.org/10.1016/s0006-8993(98)01258-x.

Dindot, S.V., Antalffy, B.A., Bhattacharjee, M.B., Beaudet, A.L., 2008. The Angelman syndrome ubiquitin ligase localizes to the synapse and nucleus, and maternal deficiency results in abnormal dendritic spine morphology. Hum. Mol. Genet. 17, 111–118. https://doi.org/10.1093/hmg/ddm288.

Gardoni, F., Caputi, A., Cimino, M., Pastorino, L., Cattabeni, F., Di Luca, M., 1998. Calcium/calmodulin-dependent protein kinase II is associated with NR2A/B subunits of NMDA receptor in postsynaptic densities. J. Neurochem. 71 (4), 1733–1741. https://doi.org/10.1046/j.1471-4159.1998.71041733.

Jana, N.R., 2012. Understanding the pathogenesis of Angelman syndrome through animal models. Neural Plast. 2012, 710943. https://doi.org/10.1155/2012/710943.

Jay, V., Becker, L.E., Chan, F.W., Perry, T.L., 1991. Puppet-like syndrome of Angelman: a pathologic and neurochemical study. Neurology 41, 416–422. https://doi.org/10.1212/wnl.41.3.416.

Jiang, Y.H., Armstrong, D., Albrecht, U., Atkins, C.M., Noebels, J.L., Eichele, G., Sweatt, J.D., Beaudet, A.L., 1998. Mutation of the Angelman ubiquitin ligase in mice causes increased cytoplasmic p53 and deficits of contextual learning and long-term potentiation. Neuron 21, 799–811. https://doi.org/10.1016/s0896-6273(00)80596-6.

Kim, H., Kunz, P.A., Mooney, R., Philpot, B.D., Smith, S.L., 2016. Maternal loss of Ube3a impairs experience-driven dendritic spine maintenance in the developing visual cortex. J. Neurosci. 36, 4888–4894. https://doi.org/10.1523/JNEUROSCI.4204-15.2016.

Koyavski, L., Panov, J., Simchi, L., Rayi, P.R., Sharvit, L., Feuermann, Y., Kaphzan, H., 2019. Sex-dependent sensory phenotypes and related transcriptomic expression profiles are differentially affected by Angelman syndrome. Mol. Neurobiol. 56, 5998–6016. https://doi.org/10.1007/s12035-019-1503-8.

Kuan, C.-Y., Burke, R.E., 2005. Targeting the JNK signaling pathway for stroke and Parkinson's diseases therapy. Curr. Drug Targets CNS Neurol. Disord. 4, 63–67.

Kuan, C.Y., Yang, D.D., Samanta Roy, D.R., Davis, R.J., Rakic, P., Flavell, R.A., 1999. The Jnk1 and Jnk2 protein kinases are required for regional specific apoptosis during early brain development. Neuron. 22 (4), 667–676. https://doi.org/10.1016/s0896-6273(00)80727-8.

Kumar, A., Singh, U.K., Kini, S.G., Garg, V., Agrawal, S., Tomar, P.K., Pathak, P., Chaudhary, A., Gupta, P., Malik, A., 2015. JNK pathway signaling: a novel and smarter therapeutic targets for various biological diseases. Future Med. Chem. 7, 2065–2086. https://doi.org/10.4155/fmc.15.132.

Okazawa, H., Estus, S., 2002. The JNK/c-Jun cascade and Alzheimer's disease. Am. J. Alzheimers Dis. Other Dement. 17, 79–88. https://doi.org/10.1177/153331750201700209.

Perrin, V., Dufour, N., Raoul, C., Hassig, R., Brouillet, E., Aebischer, P., Luthi-Carter, R., Déglon, N., 2009. Implication of the JNK pathway in a rat model of Huntington's disease. Exp. Neurol. 215, 191–200. https://doi.org/10.1016/j.expneurol.2008.10.008.

Ploia, C., Antoniou, X., Sclip, A., Grande, V., Cardinetti, D., Colombo, A., Canu, N., Benussi, L., Ghidoni, R., Forloni, G., Borsello, T., 2011. JNK plays a key role in tau hyperphosphorylation in Alzheimer's disease models. J. Alzheimers Dis. 26, 315–329. https://doi.org/10.3233/JAD-2011-110320.

Sato, M., Stryker, M.P., 2010. Genomic imprinting of experience-dependent cortical plasticity by the ubiquitin ligase gene Ube3a. Proc. Natl. Acad. Sci. U. S. A. 107, 5611–5616. https://doi.org/10.1073/pnas.1001281107.

Schellino, R., Boido, M., Borsello, T., Vercelli, A., 2018. Pharmacological c-Jun NH2-terminal kinase (JNK) pathway inhibition reduces severity of spinal muscular atrophy disease in mice. Front. Mol. Neurosci. 11, 308. https://doi.org/10.3389/fnmol.2018.00308.

Sclip, A., Antoniou, X., Colombo, A., Camici, G.G., Pozzi, L., Cardinetti, D., Feligioni, M., Veglianese, P., Bahlmann, F.H., Cervo, L., Balducci, C., Costa, C., Tozzi, A., Calabresi, P., Forloni, G., Borsello, T., 2011. c-Jun N-terminal kinase regulates soluble Aβ oligomers and cognitive impairment in AD mouse model. J. Biol. Chem. 286, 43871–43880. https://doi.org/10.1074/jbc.M111.297515.

Sclip, A., Arnaboldi, A., Colombo, I., Veglianese, P., Colombo, L., Messa, M., Mancini, S., Cimini, S., Morelli, F., Antoniou, X., Welker, E., Salmona, M., Borsello, T., 2013. Soluble Aβ oligomer-induced synaptopathy: c-Jun N-terminal kinase's role. J. Mol. Cell Biol. 5, 277–279. https://doi.org/10.1093/jmcb/mjt015.

Sclip, A., Tozzi, A., Abaza, A., Cardinetti, D., Colombo, I., Calabresi, P., Salmona, M., Welker, E., Borsello, T., 2014. c-Jun N-terminal kinase has a key role in Alzheimer disease synaptic dysfunction in vivo. Cell Death Dis. 5https://doi.org/10.1038/cddis.2013.559. e1019.

Seibenhener, M.L., Wooten, M.C., 2015. Use of the Open Field Maze to measure locomotor and anxiety-like behavior in mice. J. Vis. Exp. https://doi.org/10.3791/52434.e52434.

Vercelli, A., Biggi, S., Sclip, A., Repetto, I.E., Cimini, S., Falleroni, F., Tomasi, S., Monti, R., Tonna, N., Morelli, F., Grande, V., Stravalaci, M., Biasini, E., Marin, O., Bianco, F., di Marino, D., Borsello, T., 2015. Exploring the role of MKK7 in excitotoxicity and cerebral ischemia: a novel pharmacological strategy against brain injury. Cell Death Dis. 6, e1854. https://doi.org/10.1038/cddis.2015.226.

Wallace, M.L., Burette, A.C., Weinberg, R.J., Philpot, B.D., 2012. Maternal loss of Ube3a produces an excitatory/inhibitory imbalance through neuron type-specific synaptic defects. Neuron 74, 793–800. https://doi.org/10.1016/j.neuron.2012.03.036.

Walsh, R.N., Cummins, R.A., 1976. The open-field test: a critical review. Psychol. Bull. 83, 482–504.

Wang, W., Ma, C., Mao, Z., Li, M., 2004. JNK inhibition as a potential strategy in treating Parkinson's disease. Drug News Perspect. 17, 646–654.

Wang, S., Zhang, C., Sheng, X., Zhang, X., Wang, B., Zhang, G., 2014. Peripheral expression of MAPK pathways in Alzheimer's and Parkinson's diseases. J. Clin. Neurosci. 21, 810–814. https://doi.org/10.1016/j.jocn.2013.08.017.

Weeber, E.J., Jiang, Y.-H., Elgersma, Y., Varga, A.W., Carrasquillo, Y., Brown, S.E., Christian, J.M., Mirnikjoo, B., Silva, A., Beaudet, A.L., Sweatt, J.D., 2003. Derangements of hippocampal calcium/calmodulin-dependent protein kinase II in a mouse model for Angelman mental retardation syndrome. J. Neurosci. 23, 2634–2644.

van Woerden, G.M., Harris, K.D., Hojjati, M.R., Gustin, R.M., Qiu, S., de Avila Freire, R., Jiang, Y., Elgersma, Y., Weeber, E.J., 2007. Rescue of neurological deficits in a mouse model for Angelman syndrome by reduction of alphaCaMKII inhibitory phosphorylation. Nat. Neurosci. 10, 280–282. https://doi.org/10.1038/nn1845.

Yang, D.D., Kuan, C.Y., Whitmarsh, A.J., et al., 1997. Absence of excitotoxicity-induced apoptosis in the hippocampus of mice lacking the Jnk3 gene. Nature. 389 (6653), 865–870. https://doi.org/10.1038/39899.

Yashiro, K., Riday, T.T., Condon, K.H., Roberts, A.C., Bernardo, D.R., Prakash, R., Weinberg, R.J., Ehlers, M.D., Philpot, B.D., 2009. Ube3a is required for experience-dependent maturation of the neocortex. Nat. Neurosci. 12, 777–783. https://doi.org/10.1038/nn.2327.

Zhuo, Z.-H., Sun, Y.-Z., Jin, P.-N., Li, F.-Y., Zhang, Y.-L., Wang, H.-L., 2016. Selective targeting of MAPK family kinases JNK over p38 by rationally designed peptides as potential therapeutics for neurological disorders and epilepsy. Mol. BioSyst. 12, 2532–2540. https://doi.org/10.1039/c6mb00297h.